Published in final edited form as:
Arterioscler Thromb Vasc Biol. 2010 December ; 30(12): 2535–2543. doi:10.1161/ATVBAHA.110.214379.

MMP-2 and MMP-9 dysfunction underlie vascular stiffness in circadian clock mutant mice

Ciprian B. Anea[1], **M. Irfan Ali**[2], **Jessica M. Osmond**[2], **Jennifer C. Sullivan**[2], **David W. Stepp**[2,3], **Ana M. Merloiu**[1], and **R. Daniel Rudic**[1,†]

[1]Department of Pharmacology & Toxicology, Medical College of Georgia, Augusta, GA

[2]Vascular Biology Center, Medical College of Georgia, Augusta, GA

[3]Department of Physiology, Medical College of Georgia, Augusta, GA

Abstract

Objective—The goals in the current studies were to determine if elasticity in blood vessels is compromised in circadian clock mutant mice (Bmal1-knockout/Bmal1-KO and Per-triple knockout/Per-TKO) and if matrix metalloproteinases might confer these changes in compliance.

Methods and Results—High resolution ultrasound *in vivo* revealed impaired remodelling and increased pulse wave velocity in arteries of Bmal1-KO and Per-TKO mice. In addition, compliance of remodelled arteries and naïve, pressurized arterioles *ex vivo* from Bmal1-KO mice and Per-TKO mice was reduced, consistent with stiffening of the vascular bed. The observed vascular stiffness was coincident with dysregulation of MMP-2 and MMP-9 in Bmal1-KO mice. Further, inhibition of matrix metalloproteinases improved indices of pathological remodeling in WT mice, but the effect was abolished in Bmal1-KO mice.

Conclusions—These data reveal that circadian clock dysfunction contributes to hardening of arteries, which may involve impaired control of the extracellular matrix composition.

Introduction

The cardiovascular system is governed and characterized by 24-hour rhythms. Recent observations have begun to establish that the genetic components that underlie circadian rhythm (the circadian clock) impart a significant influence in the regulation of the vascular system. Mice with mutation of circadian clock components, including the integral component and transcription factor, Bmal1, exhibit acute vascular dysfunction[1, 2] and aberrant chronic vascular responses in angiogenesis,[3] vascular remodeling, and injury.[1]

The vascular defects in circadian mutant mice may stem, at least in part, from impairments in endothelial function.[1-4] Indeed, endothelial mediators control the structural and mechanical properties of arteries, by influencing smooth muscle cellularity but also extracellular matrix turnover to control elasticity and stiffness[5, 6] whose respective dysfunction is significantly correlated with the onset of vascular disease.[7] In the current study, we examine if elasticity in arteries and arterioles is compromised in Bmal1-KO mice and if matrix metalloproteinases might confer these changes in compliance.

† To whom correspondence should be addressed. rrudic@mcg.edu.

Conflicts of interest disclosures: There are no conflicts of interest.

Methods and materials

Animals

All experiments were conducted in accordance with the National Institutes of Health *Guide for the Care and Use of Laboratory Animals*, and approved and monitored by the Medical College of Georgia Institutional Animal Care and Use Committee. Studies were conducted in two mouse models of circadian dysfunction having distinct mutations in the circadian clock; mice with disruption of the Bmal1 gene (Bmal1-KO) and disruption of all the Period gene isoforms (Period-1, Period-2, and Period-3/Per-TKO) and respective littermate control mice were used. Mice were housed under standard 12 hour light/dark conditions (LD). Bmal1-KO and littermate wild type mice were formerly produced by gene targeting in 129Sv/J embryonic stem cells which we backcrossed 5 times to C57BL/6J. Animals were anesthetized by intraperitoneal injection (i.p.) of ketamine and xylazine.

Ultrasound Imaging

Mice were imaged in a supine position on the THM100 Mouse Pad with integrated temperature sensor, heater and ECG electrodes (Indus Instruments, Houston, TX). Appendages were secured to ECG pads to allow constant monitoring of heart rate and body temperature. Body temperature was maintained at 37.5°C. Depilatory cream (Nair™, Carter-Horner, Mississauga, ON, Canada) was used to remove fur from the region of interest and medical ultrasound acoustic gel (Other-Sonic, Pharmaceutical Innovations, Inc., Newark, NJ) was used as a coupling fluid between the real-time microvisualization (RMV) scanhead and the skin. Ultrasound imaging was performed using the Vevo 770 system (VisualSonics Inc, Toronto, Canada). Using B-mode imaging, the RMV-706 scanhead was positioned and held immobile using the VisualSonics Vevo Integrated Rail System II to view the mouse common carotids arteries (RC, LC) and heart. The RMV-706 scanhead is a 40 MHz scanhead with a 6 mm focal length and lateral and axial resolutions of 68.2 and 38.5 μm, respectively.

Pulse-wave Doppler measurement

Arterial blood flow was measured using pulse wave Doppler (PW-mode). Following a brief stabilization period, a baseline recording of pulse wave Doppler was obtained from the common carotid artery 3-4 mm before the external and internal carotid artery branch point to measure blood flow velocity. Doppler velocity measurement was made at the smallest possible angle of incidence between the Doppler beam and the assumed blood flow direction in the carotid vessel. For diameter measurement at locations where the flow velocity was measured, M-mode recording was made in the section with the targeted vessels perpendicular to the ultrasound beam. From Pulse-wave Doppler mode, peak flow velocity and velocity time interval (VTI), were calculated and averaged for three consecutive cardiac cycles. From the M-mode recording, the diameters of the vessel were measured for three cardiac cycles and averaged to an overall average vessel diameter, *D*. The total blood volume passing the measurement location per cardiac cycle flow at each location was calculated as $V = TVI^* \pi D^2/4$

Pulse wave velocity

Vascular stiffness was determined by measuring pulse wave velocity (PWV) in Pulse Wave Doppler probe. Aortic pulse wave was acquired at two aortic sites 4 cm apart (descending and abdominal aorta). All data was acquired at a depth of ~2 to 4 and ~5 to 6 mm, respectively, with the Doppler probe. PWV (in m/s) was calculated as the quotient of separation distance and the time difference between pulse arrivals, as measured from R-peaks of the ECG.

Flow Dependent Vascular Remodeling

The complete left common carotid (LC) artery ligation was performed as previously described.[8] Briefly, the distal left common carotid artery (LC) artery and its bifurcation into the external and internal carotid were exposed using blunt dissection. 8-0 nylon sutures (USSC Sutures) were used to ligate the LC artery, just proximal to the external/internal carotid artery bifurcation. Incisions were closed (5-0 suture) and the blood flow and lumen diameter were assessed using the Vevo 770 system (VisualSonics Inc, Toronto, Canada) over the next 4 weeks.

Passive mechanics studies

Common carotid arteries were excised from mice and incubated in calcium-free Krebs buffer (contents in mM: 18 NaCl, 23.8 $NaHCO_3$, 4.7 KCl, 1.2 $MgSO_4$, 1.18 KH_2PO_4, 11.1 glucose) with potassium cyanide (13mM) for one hour to deplete vessels of myogenic tone. Vessels were then mounted on the glass pipettes of a pressure myograph (Living Systems Instrumentation, Burlington, VT) in Krebs buffer heated to 37°C and gassed with 21% O_2, 5% CO_2, and 74% N_2. Intralumenal pressure was controlled by a pressure servo control via a pressure transducer. Arteries were visualized on a monitor, and lumen diameter and wall thickness were measured using a video dimension analyzer. Passive pressure response curves were conducted for right and left common carotid arteries from 0-180 mmHg in 20 mmHg increments. Circumferential stress and strain were extrapolated from pressure response curves using the following equations:

$$\text{Circumferential wall stress} = (P * ID) / 2WT$$

$$\text{Circumferential wall strain} = (ID - ID_0)/ID_0$$

ID is inner diameter, P is intralumenal pressure, WT is wall thickness, and ID_0 is inner diameter at 0 mmHg. Individual stress-strain curves were fit with an exponential regression equation in order to determine the slope coefficient, or β-coefficient, an indicator of vessel stiffness.

Histomorphometry

After 4 weeks of flow reduction induced by LC ligation, mice were anesthetized, exsanguinated, and perfused via the left ventricle with physiologic saline. In processing vascular tissues for western blotting, common carotid arteries or aortae were immediately dissected, flash frozen and stored at -80° C until further processing. In studies designated for histological or morphometric analysis of common carotid arteries, after saline infusion, mice were subsequently perfusion fixed with neutral buffered formalin. Both right and left common carotid arteries were carefully excised and post-fixed either overnight for morphometric studies or immediately embedded in frozen medium for cryotome processing using sections proximal and distal to the point of ligation. Morphometric analysis of common carotid arteries was performed using video microscopy as described. Perimeter of the vessel lumen was taken as the circumference (C) of a circle and lumen diameter (D) determined from the equation $D=C/\pi$, assuming that the vessel cross sections were circular in vivo. In order to determine stenosis area, the internal elastic lamina (IEL) and patent lumen were circumscribed to derive a radius (R) value from the formula $R=2C/\pi$, and then IEL area and luminal area (A) were calculated using the formula $A=\pi R^2$. Stenotic area was derived from the difference of IEL area and lumen area.

Batimastat treatment

Batimastat in this study was suspended in sterile PBS/0.01% Tween 80 and administered i.p. at a daily dose of 35 mg/kg (previously shown to be tolerable and effective[9]), from the day of

arterial ligation until the day of sacrifice at which time the common carotid arteries were isolated for morphometric analysis.

Gelatin Zymography

Common carotid arteries were dissected, pulverized under liquid nitrogen, and prepared with the use of zymogram sample buffer (Bio-Rad). Equal amounts of tissue homogenate from ligated left common carotid (LC) and non-ligated right common carotids (RC) were loaded on SDS-PAGE gels containing 10%gelatin (Bio-Rad). Lytic bands corresponding to molecular weights of MMP-9 and MMP-2 were observed and quantified by densitometry.

In situ gelatinase zymography

Both right and left common carotid arteries were excised and immediately embedded in frozen medium for cryotome processing. In situ zymography was performed on frozen sections with the use of EnzCheck Gelatinase/Collagenase Assay Kit (Invitrogen). Gelatinase activity was seen as an increase in fluorescence proportional to proteolytic activity. Specificity for MMPs was established by loss of signal in the presence of 1,10-phenanthroline, a general metalloproteinase inhibitor.

Murine endothelial and smooth muscle cell isolation

Aortae were isolated from 6-8 week old mice and perfused with collagenase type II (Worthington) and incubated for 60 minutes. Endothelial cells were flushed out with media and subsequently plated and cultured. The remaining aorta was cut longitudinally and in small segments and inserted in a cell culture dish plate bathed in DMEM with 10 % fetal bovine serum. After smooth muscle cells migrated onto the plate, the aortic segments were removed and the residual smooth muscle cells cultured until 80 % confluence was obtained. The murine vascular endothelial and smooth muscle cells were then lysed and subsequently used for western blotting analysis.

Western Blotting

After 4 days of complete carotid artery ligation, remodeled arteries were dissected, pulverized under liquid nitrogen, and extracted with the use of ice-cold lysis buffer. Samples were loaded on 10 % SDS-PAGE gel and transferred onto nitrocellulose membrane. MMP-9 was detected with rabbit anti-mouse MMP-9 polyclonal antibodies, followed by enhanced chemiluminescence (ECL kit, Amersham). Signals on x-ray films were quantified by use of the Image J software.

Image Analysis

Pulse wave Doppler images and M Mode diameters were digitally stored and transferred to a computer for off-line analysis. To reduce variability, imaging parameters were held constant throughout each experiment with focus and depth optimized at the beginning of the study for each animal. All studies were done using approximately the same scan plane as determined by anatomical markers.

Statistical Analysis

Statistical analysis was performed using GraphPad Prism version 4.02 for Windows (GraphPad Software, San Diego, CA). Data were compared using an ANOVA followed by a Tukey post test or an unpaired T test used as indicated. Data are expressed as mean ± SEM. P values< 0.05 were considered statistically significant.

Results

Ultrasound analysis of remodeling in Bmal1-KO mice

Chronic blood flow alteration was induced in the left common carotid artery (LC) by ligation at the external (EC) and internal carotid artery (IC) bifurcation of mice. Common carotid arteries were then visualized in vivo in anesthetized mice by ultrasound. As demonstrated in prior studies by histomorphometric quantitation of arterial cross sections,[10] ligation of the LC in wild-type mice (WT) induced inward remodeling relative to the right common carotid artery (RC) (Figure 1, top panels) as seen by a diminution in the vessel diameter imaged by ultrasound. Additionally, complete cessation of flow in the branches downstream of the ligation was confirmed as there was no detectable blood flow to image in the EC and IC downstream of the ligated LC, while in the unligated, contralateral RC, the EC and IC were clearly visible in WT mice. In Bmal1-KO mice, the LC post-ligation was enlarged relative to the response observed in WT mice. Subsequently, the time course of vascular remodeling of the lumen (inward remodeling) to ligation was monitored by ultrasound in WT and Bmal1-KO mice for 4 weeks. As early as 1 day post ligation, lumen diameter narrowed in WT mice (Figure 1B), consistent with observations describing an acute vasoconstrictive response during the process of remodeling as previously shown [11, 12]. LC lumen robustly narrowed by 4 weeks post-ligation, to 0.143 mm±0.020 from an initial diameter of 0.289 mm±0.011. Despite ligation of the LC, Bmal1-KO mice did not inward remodel (Figure 1C), with lumen diameter remaining unchanged over the 4-week time course. We further examined hemodynamics in the WT and Bmal1-KO mice. In contralateral RC, there were no major differences in transit blood volume between WT and Bmal1-KO mice (Figure 2A, B), while ligation robustly suppressed this index of blood flow, in a fashion that was comparable between WT and Bmal1-KO mice (Figure 2C, D).

Increased vascular stiffness in arteries and arterioles of Bmal1-KO and Per-TKO mice

We next assessed pulse wave velocity in naïve large arteries of Bmal1-KO and Per-TKO mice *in vivo* by assessing transit time of flow velocity waveform along in an arterial segment.[13] Pulse wave velocity was increased in aortae of Bmal1-KO (Figure 3A) and Per-TKO mice (Figure 3B). As increased pulse wave velocity is an indicator of arterial stiffness, [14, 15] we sought to more directly measure vascular compliance by assessing stress versus strain curves in *ex vivo*, pressurized conduit arteries. In these pressurized vessels, the LC inner or lumen diameter (Figure 4A) of WT mice was significantly smaller than LC of Bmal1-KO over the entire range of pressures studied, consistent with live imaging from ultrasound B-Mode imaging. In addition, wall thickness was increased in the LC of Bmal1-KO mice, relative to WT mice (Figure 4B), further evidence of an impaired inward remodeling response accompanied by medial hypertrophy in these mice with disrupted clocks. When plotting diameter versus pressure from WT mice undergoing LC ligation, the resultant stress strain curves in LCs from Bmal1-KO exhibited a leftward shift (Figure 4C) versus WT mice, indicative of a decrease in compliance. To determine if Bmal1 might also modify elasticity of blood vessels across the vascular tree, we assessed mechanical properties of resistance vessels from Bmal1-KO mice (2nd degree femoral artery blood vessels). The arterioles from Bmal1-KO mice also exhibited a leftward shift in the stress/strain curves relative to WT arterioles (Figure 4D). The derived index of vascular stiffness, the β-coefficient/elastic modulus, [16, 17] was thus increased in both remodelled LC (Figure 4E) and naïve arterioles (Figure 4F), further indication of an increase in wall stiffness in blood vessels from Bmal1-KO, that was also observed in arterioles of Per-TKO mice (Figure 5).

Matrix metalloproteinase dysfunction in Bmal1-KO mice

As the extracellular matrix exerts an important influence on the elasticity of blood vessels [18, 19] and the evolution of cardiovascular disease [20, 21], we then examined if metalloproteinase

regulation was altered in the Bmal1-KO mice. Enzyme activity examined by zymography revealed an increase an increase in MMP-2 and MMP-9 gelatin degradation with arterial ligation after 3-days of arterial ligation in the ligated LC of WT mice. The increase in MMP-9 activity was exacerbated in Bmal1-KO mice in both naïve RC and ligated LC, and also observed as an increase in MMP-2 activity in remodeled arteries. This was further reflected as an elevation in protein expression of MMP-9 (Figure 6B), MMP-2 (Figure 6C), and in situ gelatinase activity (Supplemental Figure 1) in the LC of Bmal1-KO mice relative to wild type mice. This increase in MMP-9 expression was evident throughout the vascular wall of Bmal1-KO and extended prominently to the adventitia (Supplemental Figure 2) and was also evident as increased collagen staining in the media of remodeled arteries of Bmal1-KO mice (Supplemental Figure 3). However, TIMP-1, and TIMP-2 expression (tissue inhibitors of metalloproteinases), which are constitutively produced in vascular cells, [21, 22] was not different in the remodeled and control arteries from WT and Bmal1-KO mice (data not shown). This was accompanied by an increase in cyclooxygenase-2 and an attenuation of COX-1 expression in endothelial cells (Figure 7A) while cyclooxygenase expression in vascular smooth muscle cells appeared unchanged (Figure 7B). Furthermore, inhibition of matrix metalloproteinases by administration of a synthetic inhibitor of MMPs, batimastat, reduced neointima (Figure 8A, B), stenosis (Figure 8C, Table I), and wall thickness (Figure 8D) in WT mice, but the effect was largely attenuated in Bmal1-KO mice.

Discussion

The circadian clock, a network of genes and proteins [including Bmal1, Clock, Period, and Cryptochrome genes] that control 24-hour rhythms, is emerging as an important influence in the control of the vasculature.[1-3] Bmal1-KO, Clock mutant mice, [1] and Per2 mutant mice[2] exhibit endothelial dysfunction. Moreover, the response to injury, remodeling, and angiogenesis is impaired in mice with mutation of circadian clock components.[1, 3] Herein, we demonstrate large vessel and resistance vessel stiffening in mice with genetic disruption of two distinct circadian clock components, Bmal1 and the Period isoforms. In addition, live, pulsating vessels assessed by ultrasound and pressurized vessels ex vivo corroborate our recent observations in Bmal1-KO mice observed in fixed, isolated arteries[1] to further demonstrate impairments in the response to arterial ligation, reflected as an inability to inward remodel.

In aortae of Bmal1-KO and Per-TKO mice, pulse wave velocity was increased *in vivo*. In addition, pressurized, remodeled common carotid arteries of Bmal1-KO mice *ex vivo* also exhibited a reduction in compliance relative to their counterpart WT mice, despite comparable reduction in flow in the ligated LC of WT and Bmal1-KO mice. Moreover, elasticity of remodeled arteries of WT mice was no different than their unligated contralateral vessel (data not shown). Indeed, remodeling in the 'healthy' state serves to normalize forces[23, 24] and mechanics[25] within the vasculature in face of changing hemodynamics, while pathology during flow-disturbed conditions may ensue when signaling is further compromised by compounding challenges, such as hyperlipidemia, severe hypertension, or as our data suggests—aberrant circadian rhythm. Hardening of the vasculature which was observed in the conduit arteries in naïve resistance vessels of Bmal1-KO seems to be independent of blood pressure, as Bmal1-KO mice are actually moderately hypotensive.[4, 26, 27] Indeed, the intrinsic composition of the vasculature is important in its elastic properties.

As such, the observed vascular stiffness in Bmal1-KO mice is consistent with the enhanced collagen deposition that has been demonstrated in remodeled arteries of Bmal1-KO mice.[1] Though genes relevant to the extracellular matrix have been shown to oscillate with a circadian rhythm, [28] this is the first demonstration of a defect in the matrix associated with circadian gene mutation. Both MMP-2 and MMP-9 which are important in extracellular matrix turnover were upregulated in remodeled arteries of Bmal1-KO mice. In support of a putative influence

of circadian rhythm in metalloproteinase regulation, it has been previously reported that circulating MMP-9 is elevated in the light period (relative to the dark period) in human patients with prior myocardial infarction,[29] however additional compelling evidence is scarce. Previously, we have demonstrated that Akt and nitric oxide signaling are blunted in Bmal1-KO mice,[1] which may in part contribute to the impairment in metalloproteinases.[30-32] However, the current observations also revealed that cyclooxygenase-2 was also robustly upregulated in endothelial cells of Bmal1-KO mice. Indeed, COX-2 can influence remodeling which may in part be mediated by prostanoids,[8] but may also involve metalloproteinase regulation, as has been demonstrated in transformed cells which exhibit increased MMP-2 expression in face of upregulated COX-2 expression[33] and attenuated MMP-9 expression with NSAIDs.[34] Our findings further revealed that the broad spectrum metalloproteinase inhibitor, batimastat, reduced constrictive remodeling in WT mice, while outward remodeling was enhanced in Bmal1-KO mice, improving stenosis. However, there were no effects of batimastat on neointimal area in Bmal1-KO mice, These disparate effects of batamistat on remodeling are in fact consistent with studies in pigs fed an atherogenic diet, which lacking constrictive remodeling, but are unabated in intimal hyperplasia post-balloon dilatation.[35] Future studies are needed to determine if the circadian clock directly regulates matrix deposition, and if there is a direct contribution of cyclooxygenase in the process. In conclusion, circadian clock dysfunction results in hardening of the arteries that involves impaired control of metalloproteinase expression.

Supplementary Material

Refer to Web version on PubMed Central for supplementary material.

Acknowledgments

We wish to thank Dr. David Weaver for providing Period isoform knockout mice.

We had full access to the data and take responsibility for the integrity of the data. We also all have read and agree to the manuscript as written.

Sources of Funding: This work was supported in part by grants from the National Institutes of Health (DK070658 and HL089576).

References

1. Anea CB, Zhang M, Stepp DW, Simkins GB, Reed G, Fulton DJ, Rudic RD. Vascular disease in mice with a dysfunctional circadian clock. Circulation 2009;119:1510–1517. [PubMed: 19273720]
2. Viswambharan H, Carvas JM, Antic V, Marecic A, Jud C, Zaugg CE, Ming XF, Montani JP, Albrecht U, Yang Z. Mutation of the circadian clock gene Per2 alters vascular endothelial function. Circulation 2007;115:2188–2195. [PubMed: 17404161]
3. Wang CY, Wen MS, Wang HW, Hsieh IC, Li Y, Liu PY, Lin FC, Liao JK. Increased vascular senescence and impaired endothelial progenitor cell function mediated by mutation of circadian gene Per2. Circulation 2008;118:2166–2173. [PubMed: 18981300]
4. Westgate EJ, Cheng Y, Reilly DF, Price TS, Walisser JA, Bradfield CA, FitzGerald GA. Genetic components of the circadian clock regulate thrombogenesis in vivo. Circulation 2008;117:2087–2095. [PubMed: 18413500]
5. Kinlay S, Creager MA, Fukumoto M, Hikita H, Fang JC, Selwyn AP, Ganz P. Endothelium-derived nitric oxide regulates arterial elasticity in human arteries in vivo. Hypertension 2001;38:1049–1053. [PubMed: 11711496]
6. Ramsey MW, Goodfellow J, Jones CJH, Luddington LA, Lewis MJ, Henderson AH. Endothelial Control of Arterial Distensibility is Impaired in Chronic Heart-Failure. Circulation 1995;92:3212–3219. [PubMed: 7586306]

7. Sutton-Tyrrell K, Najjar SS, Boudreau RM, Venkitachalam L, Kupelian V, Simonsick EM, Havlik R, Lakatta EG, Spurgeon H, Kritchevsky S, Pahor M, Bauer D, Newman A, Hlth ABCS. Elevated aortic pulse wave velocity, a marker of arterial stiffness, predicts cardiovascular events in well-functioning older adults. Circulation 2005;111:3384–3390. [PubMed: 15967850]
8. Rudic RD, Brinster D, Cheng Y, Fries S, Song WL, Austin S, Coffman TM, FitzGerald GA. COX-2-derived prostacyclin modulates vascular remodeling. Circ Res 2005;96:1240–1247. [PubMed: 15905461]
9. Wang X, Fu X, Brown PD, Crimmin MJ, Hoffman RM. Matrix Metalloproteinase Inhibitor Bb-94 (Batimastat) Inhibits Human Colon-Tumor Growth and Spread in a Patient-Like Orthotopic Model in Nude-Mice. Cancer Research 1994;54:4726–4728. [PubMed: 8062271]
10. Harmon KJ, Couper LL, Lindner V. Strain-Dependent Vascular Remodeling Phenotypes in Inbred Mice. Am J Pathol 2000;156:1741–1748. [PubMed: 10793085]
11. Rudic RD, Bucci M, Fulton D, Segal SS, Sessa WC. Temporal events underlying arterial remodeling after chronic flow reduction in mice: correlation of structural changes with a deficit in basal nitric oxide synthesis. Circ Res 2000;86:1160–1166. [PubMed: 10850968]
12. Langille BL, Bendeck MP, Keeley FW. Adaptations of carotid arteries of young and mature rabbits to reduced carotid blood flow. Am J Physiol 1989;256:H931–939. [PubMed: 2705563]
13. Sikka G, Yang R, Reid S, Benjo A, Koitabashi N, Camara A, Baraban E, O'Donnell CP, Berkowitz DE, Barouch LA. Leptin is essential in maintaining normal vascular compliance independent of body weight. Int J Obes (Lond) 34:203–206. [PubMed: 19806156]
14. Asmar R, Benetos A, Topouchian J, Laurent P, Pannier B, Brisac AM, Target R, Levy BI. Assessment of Arterial Distensibility by Automatic Pulse-Wave Velocity-Measurement - Validation and Clinical-Application Studies. Hypertension 1995;26:485–490. [PubMed: 7649586]
15. Avolio AP, Chen SG, Wang RP, Zhang CL, Li MF, Orourke MF. Effects of Aging on Changing Arterial Compliance and Left-Ventricular Load in A Northern Chinese Urban-Community. Circulation 1983;68:50–58. [PubMed: 6851054]
16. Baumbach GL, Didion SP, Faraci FM. Hypertrophy of cerebral arterioles in mice deficient in expression of the gene for CuZn superoxide dismutase. Stroke 2006;37:1850–1855. [PubMed: 16763183]
17. Rigsby CS, Pollock DM, Dorrance AM. Spironolactone improves structure and increases tone in the cerebral vasculature of male spontaneously hypertensive stroke-prone rats. Microvasc Res 2007;73:198–205. [PubMed: 17250855]
18. Zieman SJ, Melenovsky V, Kass DA. Mechanisms, pathophysiology, and therapy of arterial stiffness. Arteriosclerosis Thrombosis and Vascular Biology 2005;25:932–943.
19. Intengan HD, Schiffrin EL. Structure and mechanical properties of resistance arteries in hypertension - Role of adhesion molecules and extracellular matrix determinants. Hypertension 2000;36:312–318. [PubMed: 10988257]
20. Galis ZS, Muszynski M, Sukhova GK, Simonmorrissey E, Unemori EN, Lark MW, Amento E, Libby P. Cytokine-Stimulated Human Vascular Smooth-Muscle Cells Synthesize a Complement of Enzymes Required for Extracellular-Matrix Digestion. Circulation Research 1994;75:181–189. [PubMed: 8013077]
21. Galis ZS, Sukhova GK, Lark MW, Libby P. Increased Expression of Matrix Metalloproteinases and Matrix-Degrading Activity in Vulnerable Regions of Human Atherosclerotic Plaques. Journal of Clinical Investigation 1994;94:2493–2503. [PubMed: 7989608]
22. Zhang JS, Nie L, Razavian M, Ahmed M, Dobrucki LW, Asadi A, Edwards DS, Azure M, Sinusas AJ, Sadeghi MM. Molecular Imaging of Activated Matrix Metalloproteinases in Vascular Remodeling. Circulation 2008;118:1953–1960. [PubMed: 18936327]
23. Glagov S, Weisenberg E, Zarins CK, Stankunavicius R, Kolettis GJ. Compensatory enlargement of human atherosclerotic coronary arteries. N Engl J Med 1987;316:1371–1375. [PubMed: 3574413]
24. Kamiya A, Togawa T. Adaptive regulation of wall shear stress to flow change in the canine carotid artery. Am J Physiol 1980;239:H14–21. [PubMed: 7396013]
25. Intengan HD, Deng LY, Li JS, Schiffrin EL. Mechanics and composition of human subcutaneous resistance arteries in essential hypertension. Hypertension 1999;33:569–574. [PubMed: 9931167]

26. Curtis AM, Cheng Y, Kapoor S, Reilly D, Price TS, Fitzgerald GA. Circadian variation of blood pressure and the vascular response to asynchronous stress. Proc Natl Acad Sci U S A 2007;104:3450–3455. [PubMed: 17360665]
27. Rudic RD, Fulton DJ. Pressed for time: the circadian clock and hypertension. J Appl Physiol 2009;107:1328–1338. [PubMed: 19679741]
28. Rudic RD, McNamara P, Reilly D, Grosser T, Curtis AM, Price TS, Panda S, Hogenesch JB, FitzGerald GA. Bioinformatic analysis of circadian gene oscillation in mouse aorta. Circulation 2005;112:2716–2724. [PubMed: 16230482]
29. Dominguez-Rodriguez A, Abreu-Gonzalez P, Garcia-Gonzalez MJ, Reiter RJ. Relation of nocturnal melatonin levels to serum matrix metalloproteinase-9 concentrations in patients with myocardial infarction. Thromb Res 2007;120:361–366. [PubMed: 17126384]
30. Aicher A, Heeschen C, Mildner-Rihm C, Urbich C, Ihling C, Technau-Ihling K, Zeiher AM, Dimmeler S. Essential role of endothelial nitric oxide synthase for mobilization of stem and progenitor cells. Nature Medicine 2003;9:1370–1376.
31. Kim D, Kim S, Koh H, Yoon SO, Chung AS, Cho KS, Chung J. Akt/PKB promotes cancer cell invasion via increased motility and metalloproteinase production. Faseb Journal 2001;15:1953–1962. [PubMed: 11532975]
32. Mangi AA, Noiseux N, Kong DL, He HM, Rezvani M, Ingwall JS, Dzau VJ. Mesenchymal stem cells modified with Akt prevent remodeling and restore performance of infarcted hearts. Nature Medicine 2003;9:1195–1201.
33. Tsujii M, Kawano S, DuBois RN. Cyclooxygenase-2 expression in human colon cancer cells increases metastatic potential. Proceedings of the National Academy of Sciences of the United States of America 1997;94:3336–3340. [PubMed: 9096394]
34. Murono S, Yoshizaki T, Sato H, Takeshita H, Furukawa M, Pagano JS. Aspirin inhibits tumor cell invasiveness induced by Epstein-Barr virus latent membrane protein 1 through suppression of matrix metalloproteinase-9 expression. Cancer Res 2000;60:2555–2561. [PubMed: 10811139]
35. de Smet BJGL, de Kleijn D, Hanemaaijer R, Verheijen JH, Robertus L, van der Helm YJM, Borst C, Post MJ. Metalloproteinase Inhibition Reduces Constrictive Arterial Remodeling After Balloon Angioplasty : A Study in the Atherosclerotic Yucatan Micropig. Circulation 2000;101:2962–2967. [PubMed: 10869270]

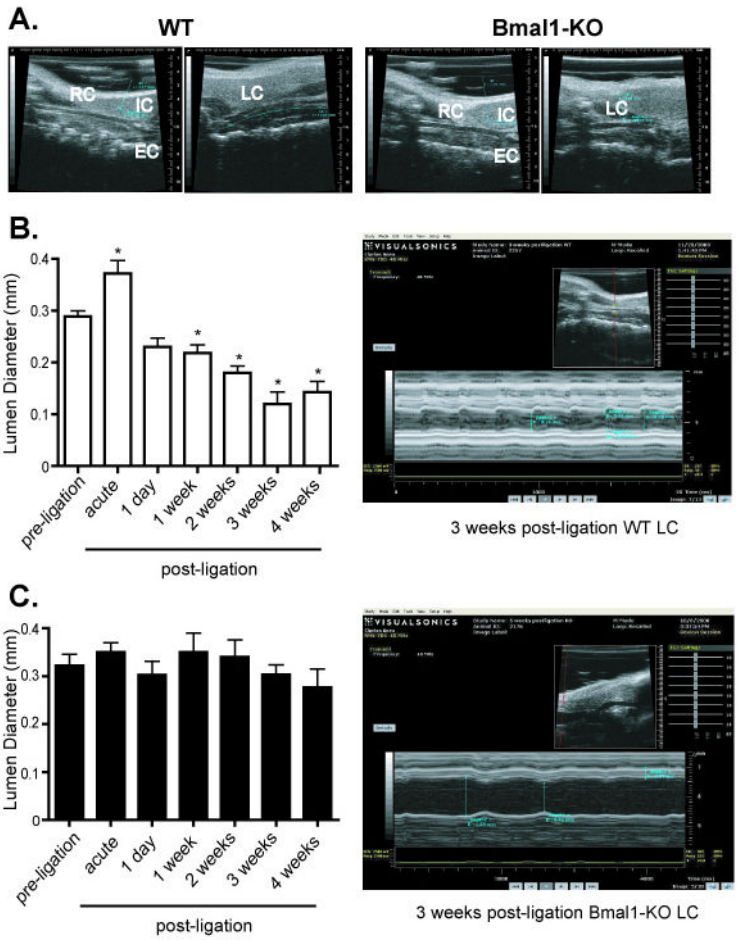

Figure 1. Ultrasound analysis of vascular remodeling in WT and Bmal1-KO mice

A. The common carotid artery was visualized through echo ultrasound imaging using B Mode (see methods). Typical vascular remodelling evident as a lumen reduction was evident after 4 weeks of arterial ligation in male, wild-type mice (left two panels), Bmal1-KO mice exhibited no change in diameter or a paradoxical increase diameter (right two panels). In the unligated RC, the EC and IC were clearly visible, but absent in the ligated LC in WT and Bmal1-KO mice. **B.** Ultrasound imaging using M-Mode (see methods) was used to observe the common carotid artery of WT mice after 1 day to 4 weeks of ligation. End diastolic lumen diameter was measured as an index of live *in vivo* vascular remodelling. Even after 1 day of arterial ligation, a reduction in lumen diameter was observed that progressed through 4 weeks post-ligation in WT mice (right top panel). **C.** Bmal1-KO mice exhibited no change in diameter (right bottom panel) (N= 6/ group, *p<0.05 by one-way ANOVA versus corresponding preligation lumen diameter)

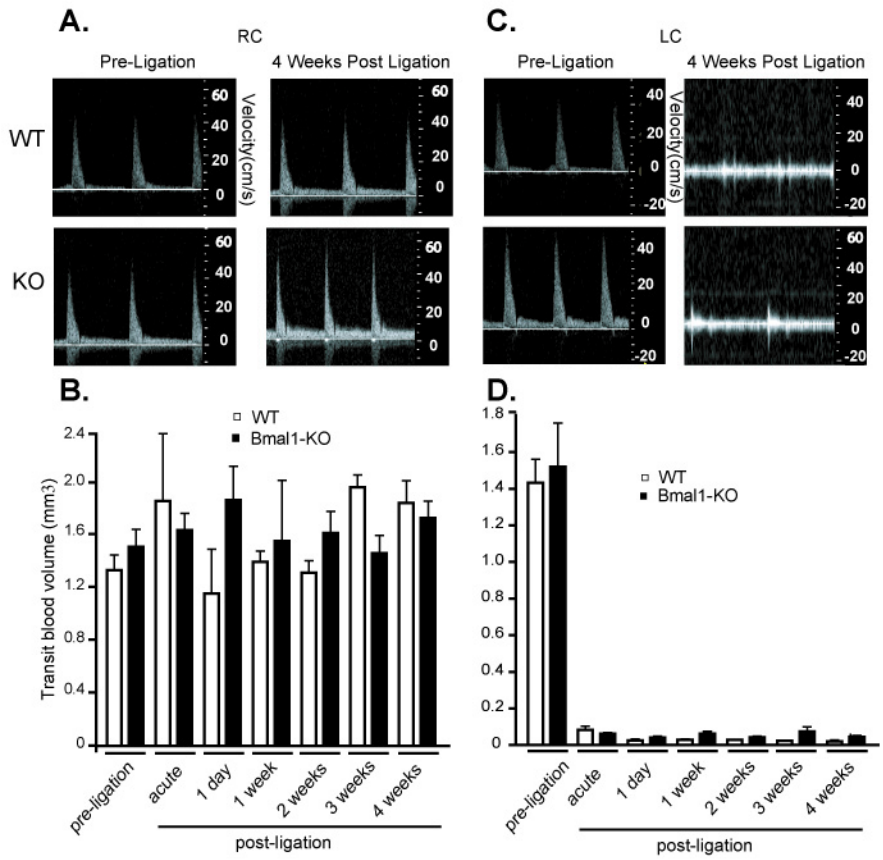

Figure 2. Flow velocity and transit blood flow volume in WT and Bmal1-KO mice

Doppler flow velocity in common carotid arteries was determined by echo ultrasound using PWD Mode imaging (see methods) in RC (**A**) and LC pre- and 4 weeks post-ligation (**C**). Transit blood flow was then determined in the RC (**B**) and LC (**D**) in weekly intervals to 4 weeks post-ligation. **B.** Contralateral, unligated RC did not display significant changes in WT versus Bmal1-KO mice before nor after the surgical ligation of LC (N=6/group). **D.** Blood flow in LC artery underwent a dramatic drop after ligation which was constant and not different in WT versus Bmal1-KO mice over the course of 4 weeks after ligation (N=6/group).

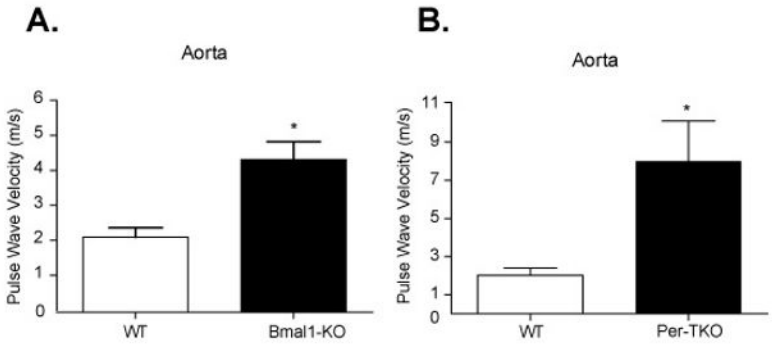

Figure 3. Increased pulse wave velocity in the great arteries of Bmal1-KO mice

Pulse wave velocity was assessed noninvasively by ultrasound (see methods) in the aortae of (**A**) Bmal1-KO and (**B**) Per triple KO mice (N=4 *p<0.05, unpaired T test).

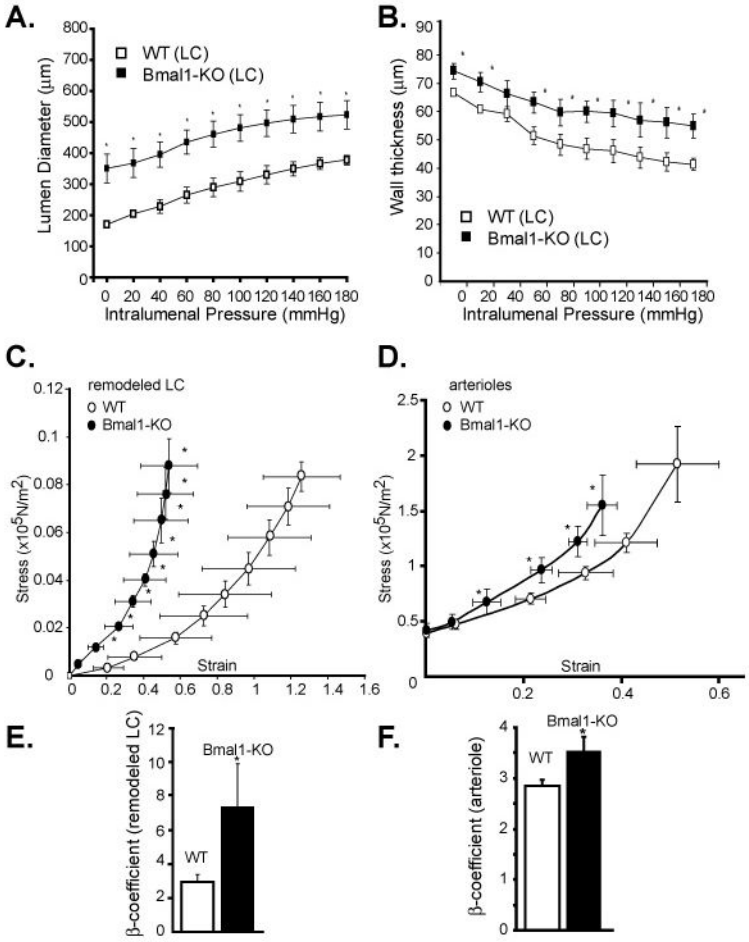

Figure 4. Increased vascular stiffness in remodelled arteries and arterioles of Bmal1-KO mice

A. Pressure-diameter relationships were assessed *ex vivo* in remodelled left common carotid arteries 4 weeks after ligation. **B.** Wall thickness was also assessed in the remodelled LC arteries (N = 4–7). **C.** Circumferential wall stress and strain were calculated from measurements made over a range of pressures in passive, calcium-free conditions. Arteries were preincubated for 1 hour in KCN 13μM solution to eliminate the myogenic tone. In the LC undergoing 4 weeks of ligation of Bmal1-KO mice, there was a leftward shift in the stress/strain curve, indicating a decrease in LC compliance. **D.** Arterioles in proximity to the femoral artery were also isolated and stress/strain curves determined, indicating a decrease in compliance in Bmal1-KO mice. Beta-coefficients derived from stress/strain relationships were significantly increased in the remodelled arteries (**E**) and arterioles (**F**) of Bmal1 KO mice (*$p<0.05$, N=5 for LC's from Bmal1 KO mice, N=7 for control WT (*$p<0.05$; n=5 for Bmal1 KO mice, N=7 for WT).

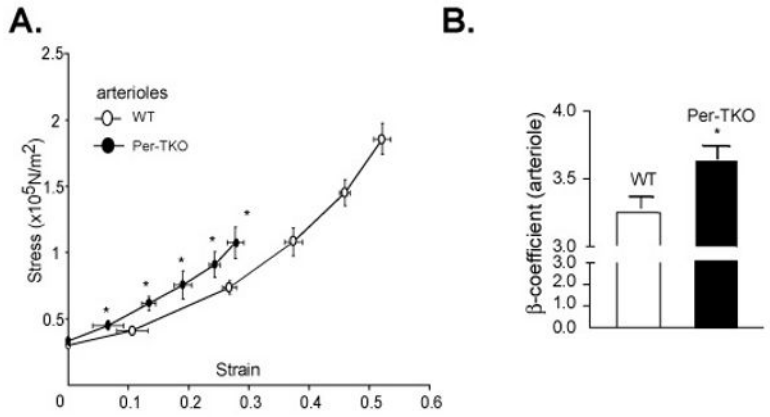

Figure 5. Increased vascular stiffness in arterioles of Per triple KO mice

(**A**) Circumferential wall stress and strain were determined in isolated arterioles proximal to the femoral artery from Per triple KO mice. Beta-coefficients derived from stress/strain relationships were significantly increased (**B**) (*$p<0.05$, N=6)

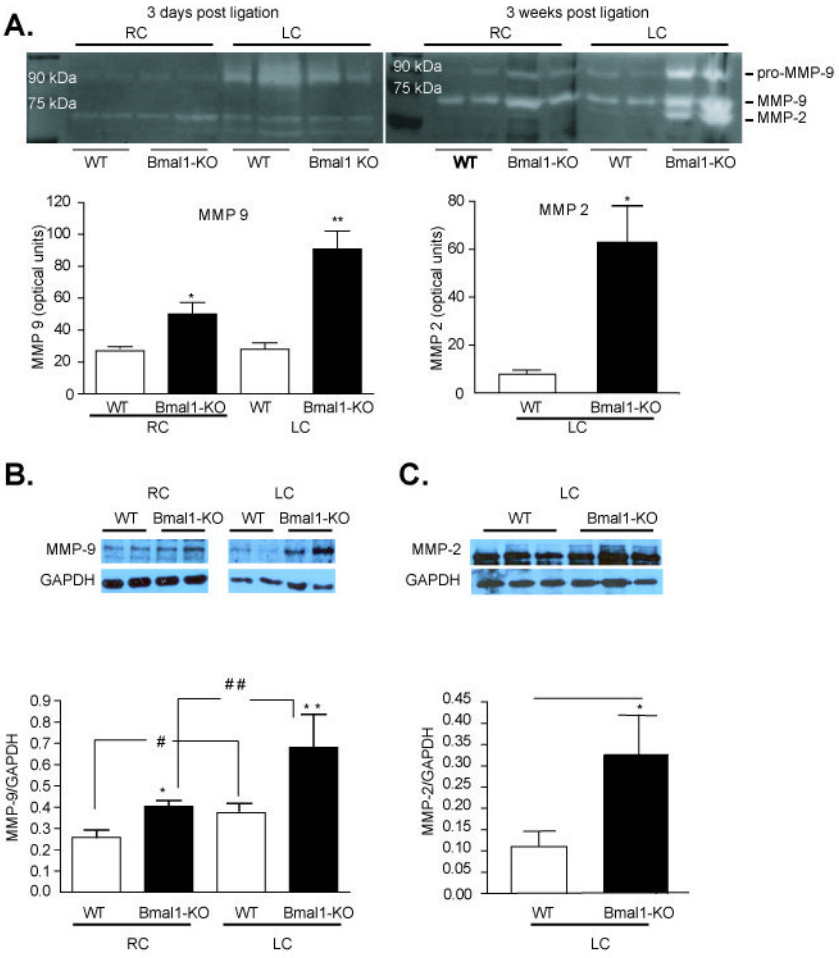

Figure 6. Increased expression and activity of MMP-9 and MMP-2 in Bmal1 KO mice

Increased gelatinolytic activity in carotid artery post ligation. Equal amounts of tissue homogenate were loaded on SDS-PAGE gels containing gelatine. (**A**) Gelatinolytic activity associated with MMP-9 was equally induced at day 3 after ligation in both Bmal1-KO and WT ligated common carotid arteries. After 3 weeks of ligation gelatinolytic activity associated with MMP-9 and MMP-2 was significantly increased in Bmal1-KO compared to WT littermate controls (N=4) Remodelled arteries were dissected and protein lysates were isolated and separated by SDS-PAGE electrophoresis from littermate control wild-type mice versus Bmal1-KO mice at a single time point (12 PM). Expression levels of MMP-9 (**B**) and MMP-2 (**C**) were significantly increased in remodelled left common carotid arteries relative to wild-type mice. Changes were quantified by densitometry (*p<0.05 versus WT). (N=4 Wild-type, N=4 Bmal1-KO)

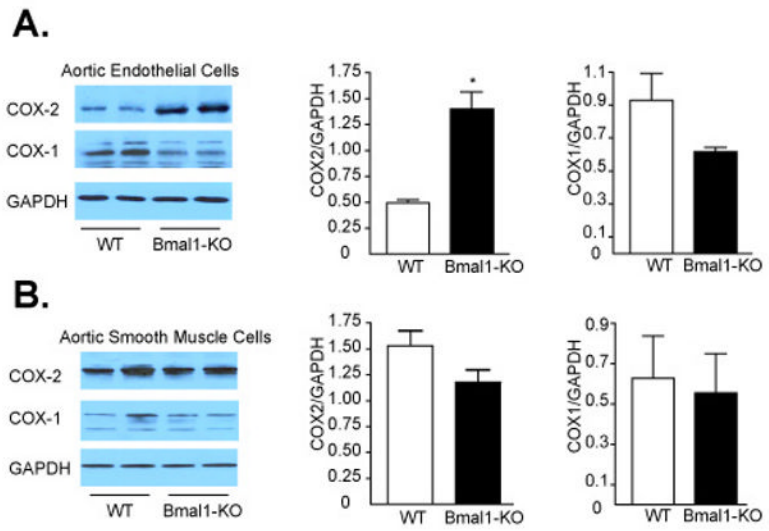

Figure 7. Increased COX 2 expression in Bmal1-KO endothelial cells

Mouse aortic endothelial and smooth muscle cells were isolated from Bmal1-KO and WT mice (see methods). Isolated cells were cultured and protein lysates were isolated and separated by SDS-PAGE electrophoresis. (**A**) Expression levels of COX-2 but not COX-1 were significantly increased in endothelial cells from Bmal1-KO mice. (**B**) COX-2 and COX -1were not significantly different in isolated smooth muscle cells from Bmal1-KO and WT control mice. Changes were quantified by densitometry (*$p<0.05$ versus WT; N=6)

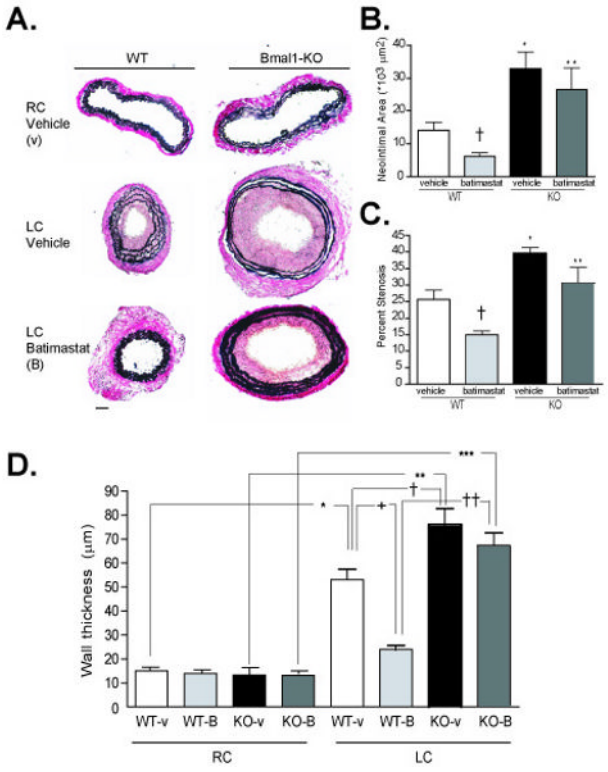

Figure 8. Impaired response to batimastat in Bmal1-KO mice

A. Von Gieson staining of elastin fibers revealed enhanced intimal hyperplasia in the left common carotid artery of Bmal1-KO mice undergoing LC ligation for 4 weeks. Neointima formation and wall thickening was partly prevented in WT mice administered batimastat. Neointimal area, wall thickness, and lumen diameter were calculated by morphometry of cross sections (see methods). Typical vascular remodeling evident as a lumen reduction was evident after 4 weeks of arterial ligation in wild-type mice, while Bmal1-KO mice exhibited no change in diameter. Analysis revealed an increase in neointimal area (**B)** and percent stenosis (**C**) in Bmal1-KO mice administered vehicle i.p. (N=3 *p<0.05). Neointima formation and stenosis were reduced in batimastat-treated WT mice compared to vehicle-treated WT ((N=3 *p<0.05, unpaired T test) while this effect was abrogated in Bmal1-KO mice. Wall thickness (**D)** (calculated at the level of EEL) was increased in both WT and Bmal1-KO ligated LC compared to RC control with the LC Bmal1-KO being significantly larger than the control LC WT. Batimastat treatment significantly reduced media thickness in LC WT compared to vehicle control LC WT, but again did not have any significant effect in LC of Bmal1 KO treated mice (N=3 *p<0.05, one-way ANOVA, Tukey post-test).

Table 1

Effect of Batimastat on lumen diameter during remodeling in Bmal1-KO mice

End diastolic lumen diameter was measured live in vivo through echo ultrasound imaging using M-Mode (see methods). Vascular remodelling evident as a lumen diameter reduction was evident by 1 week post-arterial ligation in wild-type mice, treated with vehicle control (LC remodeling, top table). Batimastat treatment in WT mice accelerated a constrictive response demonstrated as a significant reduction in lumen diameter, 1 day post-ligation. However, by 3 weeks after the ligation, constrictive remodeling in LC WT treated with Batimastat was attenuated, exhibiting increased lumen diameter compared to LC WT mice treated with vehicle (N= 4/ group, *p<0.05 by unpaired T-test). Bmal1-KO mice exhibited no inward remodeling, but exhibited outward remodeling which was significant at 2 weeks in the vehicle administrated group and in an analogous manner to WT, became accelerated, albeit outward, occurring with significance at 4 days and 2 weeks post-ligation in the Batimastat treated group (top table) (N= 4/ group, *p<0.05 by one-way ANOVA versus corresponding preligation lumen diameter). Batimastat and Bmal1 mutation did not affect lumen diameter in control, contralateral RC (bottom table).

LC (mm)	Pre-ligation	1 Day Post-ligation	4 Days Post-ligation	1 Week Post-ligation	2 Weeks Post-ligation	3 Weeks Post-ligation
WT Vehicle	0.30 +/- 0.016	0.26+/- 0.022	0.26+/- 0.016	0.25+/- 0.005 *	0.21+/- 0.007 *	0.16+/- 0.012 *
WT Batimastat	0.29+/- 0.015	0.23+/- 0.007 *	0.17+/- 0.008 *	0.2+/- 0.004 *	0.17+/- 0.009 *	0.2+/- 0.012 *†
KO Vehicle	0.30+/- 0.015	0.29+/- 0.011	0.34+/- 0.009	0.36+/- 0.009	0.39+/- 0.029 #	0.35+/- 0.042
KO Batimastat	0.29+/- 0.007	0.27+/- 0.012	0.38+/- 0.007 #	0.37+/- 0.021	0.39+/- 0.007 #	0.35+/- 0.017
RC (mm)	Pre-ligation	1 Day Post-ligation	4 Days Post-ligation	1 Week Post-ligation	2 Weeks Post-ligation	3 Weeks Post-ligation
WT Vehicle	0.28+/- 0.012	0.28+/- 0.009	0.31+/- 0.01	0.31+/- 0.012	0.31+/- 0.011	0.29+/- 0.015
WT Batimastat	0.28+/- 0.019	0.27+/- 0.008	0.27+/- 0.005	0.27+/- 0.012	0.26+/- 0.003	0.27+/- 0.007
KO Vehicle	0.31+/- 0.016	0.32+/- 0.005	0.32+/- 0.005	0.33+/- 0.021	0.34+/- 0.036	0.33+/- 0.012
KO Batimastat	0.31+/- 0.016	0.32+/- 0.005	0.33+/- 0.016	0.33+/- 0.019	0.33+/- 0.037	0.31+/- 0.015